

Extended x-ray-absorption fine-structure Debye-Waller factors and vibrational density of states in amorphous arsenic

P. P. Lottici

Dipartimento di Fisica, Università degli Studi di Parma, Parma, Italy

(Received 13 June 1986; revised manuscript received 7 October 1986)

A connection between Raman intensities and the extended x-ray-absorption fine-structure (EXAFS) nearest-neighbor mean-square relative displacement σ_R^2 , stressing the predominance of bond-compression mechanisms in depolarized Raman scattering, is tested in amorphous arsenic. Parameter-free relative densities of states, which enter σ_R^2 calculations, are obtained from the reduced Raman intensity and from neutron inelastic scattering data, in the framework of a nearest-neighbor central-force model. In both cases, the experimental temperature dependence of the EXAFS Debye-Waller thermal disorder parameter is well reproduced. The results are discussed in terms of Einstein and Debye models through a calculation of the negative moments of the relative density of states.

INTRODUCTION

Very few authors¹⁻⁶ have faced the problem of extracting information on vibrational dynamics from EXAFS (extended x-ray absorption fine structure) data: generally the main purpose in interpreting EXAFS spectra is to obtain structural information and therefore a limited discussion is devoted to the lattice dynamics affecting the EXAFS spectra through a Debye-Waller-like factor $\exp(-2k^2\sigma_R^2)$. In a previous paper,⁵ we connected the Raman scattering intensities with the Debye-Waller parameter σ_R^2 which appears in the EXAFS of tetrahedrally coordinated amorphous semiconductors. The connection is based on the simple idea that the bond-stretching motion of the atoms, which contributes to the reduced Raman intensity, is essentially the vibrational mechanism determining the EXAFS Debye-Waller factors. In this work we extend this Raman-EXAFS connection to the threefold-coordinated amorphous arsenic whose EXAFS Debye-Waller parameter temperature dependence has been measured and reported previously.⁷

EXAFS DEBYE-WALLER PARAMETER

The EXAFS is an important technique for determining the local structure around absorbing atoms both in crystalline and disordered solids.⁸ The usefulness of EXAFS measurements is based on the simple parametrization of the EXAFS modulation $\chi(k)$ in terms of structural quantities as interatomic distances R and coordination numbers N of the shells:

$$\chi(k) = - \sum_R \frac{N_R f_R}{kR^2} \sin(2kR + \delta_R) \exp(-2R/\lambda_R) \times \exp(-2k^2\sigma^2). \quad (1)$$

Other quantities in Eq. (1) are the backscattering amplitudes f_R , the phase shifts δ_R , and the electron mean free

paths λ_R . k is the photoelectron wave number. Current EXAFS theories assume that the static disorder and the temperature dependence of the EXAFS oscillations can be well described by a Debye-Waller-like factor $\exp(-2k^2\sigma^2)$, at least in nonpathological cases⁹ (i.e., when the radial distribution function around the absorbing atom is symmetric and/or when anharmonic effects are negligible). A knowledge of σ^2 is important for accurate determination of coordination numbers from EXAFS data and, on the other hand, its temperature dependence gives information on the relative importance of structural and thermal disorder.²

The thermal contribution to the Debye-Waller factor is determined by the mean-square relative displacement (MSRD) σ_R^2 of the central absorbing atom relative to its neighbors. The MSRD for a pair of atoms at sites l and l' is defined by

$$\sigma_R^2 = \langle [(\mathbf{u}_l - \mathbf{u}_{l'}) \cdot \hat{\mathbf{R}}_{ll'}]^2 \rangle, \quad (2)$$

where \mathbf{u}_l is the displacement vector of the atom at site l from its equilibrium position, $\hat{\mathbf{R}}_{ll'}$ is a unit vector in the direction $l-l'$ and $\langle \rangle$ denotes a thermal average.

The MSRD is then the mean-square compression of the bond between atoms at l and l'

$$\sigma_R^2 = \langle c_R^2 \rangle, \quad (3)$$

where $c_R = (\mathbf{u}_l - \mathbf{u}_{l'}) \cdot \hat{\mathbf{R}}_{ll'}$.

Sevillano *et al.*³ have shown that in fcc materials an Einstein model gives an accurate description of the temperature dependence of the MSRD of nearest neighbors. In this model the nearest neighbor MSRD is given by

$$\sigma_R^2 = \frac{\hbar}{2\mu\omega_E} \coth \left[\frac{\hbar\omega_E}{2k_B T} \right], \quad (4)$$

where μ is the reduced mass for the atom pair (l, l') and ω_E is the Einstein frequency.

ω_E is usually taken as a parameter to be determined from best fitting procedures and the obtained values may

have some physical meaning. Very recently, Knapp *et al.*⁶ have shown that the Einstein parameter obtained in a series of fcc metals is equal to the square root of the second moment of the phonon density of states, as determined from heat capacity data.

This result may be explained in a direct way in the nearest-neighbor central-force (NN-CF) approximation because the MSRD then depends only on the NN-CF constant and can be expressed in terms of the normalized phonon density of states (DOS) $\rho(\omega)$:

$$\sigma_R^2 = \frac{\hbar}{M\omega^2} \int \rho(\omega) \omega \coth \left[\frac{\hbar\omega}{2k_B T} \right] d\omega, \quad (5)$$

$\overline{\omega^2} = \int \rho(\omega) \omega^2 d\omega$ being the second moment of the frequency spectrum and M the mass of the atoms.

In the low- and high-temperature limits we have

$$\sigma_R^2 \simeq \begin{cases} \frac{\hbar\overline{\omega}}{M\omega^2} & \text{at low } T \\ \frac{2k_B T}{M\omega^2} & \text{at high } T, \end{cases} \quad (6)$$

i.e., σ_R^2 is T independent at low temperatures and linear with T at high temperatures. The Einstein model [Eq. (4)] will reproduce Eq. (6) provided that

$$\omega_E = \begin{cases} \frac{\overline{\omega^2}}{\overline{\omega}} & \text{at low } T \\ (\overline{\omega^2})^{1/2} & \text{at high } T. \end{cases} \quad (7)$$

The Einstein frequency appropriate for EXAFS may then be expressed, in the NN-CF approximation, by means of the first positive moments of the total density of states (DOS). In this derivation, a crystalline lattice is not required: by introducing a configurational average, equivalent results are valid for monatomic amorphous solids.

A rough estimate of the moments of the total DOS can be given by the Debye approximation, where $\rho(\omega) = 3\omega^2/\omega_D^3$, ω_D being the Debye cutoff frequency:

$$\omega_E = \begin{cases} \frac{4}{5}\omega_D & \text{at low } T \\ \sqrt{\frac{3}{5}}\omega_D & \text{at high } T, \end{cases} \quad (8)$$

then $\omega_E = 0.787\omega_D$ should produce the best fit to Debye-like data.

RELATIVE DENSITY OF STATES (RDOS)

The MSRD σ_R^2 may be expressed^{3,5,10} in terms of a relative (also called local or projected) density of vibrational states $\rho_R(\omega)$ to which only the modes giving rise to relative motion, i.e., to compression of the bonds, contribute:

$$\sigma_R^2 = \frac{\hbar}{2\mu} \int \frac{\rho_R(\omega)}{\omega} \coth \left[\frac{\hbar\omega}{2k_B T} \right] d\omega. \quad (9)$$

By comparison of Eqs. (9) and (5) we find the important

result⁵ that in the NN-CF model the RDOS is simply connected with the normalized DOS $\rho(\omega)$

$$\rho_R(\omega) = \frac{\omega^2}{\overline{\omega^2}} \rho(\omega). \quad (10)$$

We then have a way to relate the RDOS to the phonon spectrum and its moments. By measuring the temperature dependence of the EXAFS Debye-Waller factor we could check, for example, the validity of NN-CF models.

At low temperatures Eq. (9) gives

$$\sigma_R^2 \simeq \frac{\hbar}{M} (\overline{\omega^{-1}})_R \quad \text{at low } T, \quad (11a)$$

whereas at high temperatures

$$\sigma_R^2 \simeq \frac{2k_B T}{M} (\overline{\omega^{-2}})_R \quad \text{at high } T, \quad (11b)$$

where the negative moments $(\overline{\omega^{-n}})_R$ are calculated with respect to the RDOS. When Eq. (10) applies, we obviously recover the results given in Eq. (6).

The Einstein frequency appropriate for EXAFS is then intermediate between $(\overline{\omega^{-1}})_R^{-1}$ and $(\overline{\omega^{-2}})_R^{-1/2}$. These moments can be calculated, for example, in the Debye model.^{1,3,7,10} The RDOS for an isotropic lattice in the correlated Debye model is

$$\rho_R^D(\omega) = \frac{3\omega^2}{\omega_D^3} \left[1 - \frac{\sin \frac{\omega R}{x}}{\frac{\omega R}{x}} \right], \quad (12)$$

where $x = \omega_D / (6\pi^2 \rho / M)^{1/3}$, ρ being the density. One then obtains

$$(\overline{\omega^{-1}})_R = \frac{2}{3\omega_D} \left[1 - \left[\frac{\sin \frac{\omega_D R}{x}}{\frac{\omega_D R}{x}} \right]^2 \right], \quad (13a)$$

$$(\overline{\omega^{-2}})_R = \frac{3}{\omega_D^2} \left[1 - \frac{\text{si} \left[\frac{\omega_D R}{x} \right]}{\frac{\omega_D R}{x}} \right], \quad (13b)$$

si being the sine-integral function.¹⁰

In the following we will discuss the case of the amorphous arsenic and we will compare the results for the temperature dependence of σ_R^2 , calculated by means of Eq. (9) in the Einstein [Eq. (4)] and correlated Debye [Eq. (12)] approximations, with those obtained from reduced density of states as given by Raman spectra or by neutron inelastic scattering data.

AMORPHOUS As

The stable structures of amorphous and crystalline As are all based on similar four atom molecular units. In the condensed state, the regular As_4 molecule of gaseous As distorts into a flattened pyramidal shape. The bond length remains practically the same but the bond angle in-

creases from 60° to about 98° . In crystalline arsenic, neighboring units are bound together in opposite senses, so that double layers of atoms are generated.¹¹

Amorphous arsenic can be prepared in a variety of densities, ranging from 4.3 to 5.2 g/cm³, which are generally lower than that of crystalline arsenic. The lower density results in a lowering of the interlayer correlations and a continuous random network (CRN) is formed.¹¹ The CRN models commonly used for calculations consist of maintaining a constant bond length, restraining the bond angle to within 10° of the average value and allowing the dihedral angle (i.e., the angle that specifies the relative orientation of two neighboring bonds) to take any value necessary to achieve connectivity.

The distribution of phonon states in amorphous arsenic has been obtained by Leadbetter *et al.*¹² from the inelastic scattering of neutrons and is reproduced in Fig. 1. The spectrum consists of two broad peaks of almost equal area that can be attributed to acoustic and optical modes. These modes can be more usefully identified as bond-bending and bond-stretching modes, respectively.¹¹ The upper optical peak is at about 230 cm^{-1} . The two-peaked structure of the phonon DOS of arsenic (both in crystalline and in amorphous form) has been qualitatively explained by Lucovsky and Knights¹³ using a valence force model. They assumed that the normal vibrational modes of an As₄ pyramidal molecule are also characteristic of the solid phase with some modification of the bending and stretching frequencies.

Beeman and Alben,¹⁴ using equation-of-motion methods, obtained the distribution of phonon states in amorphous arsenic for CRN models, reproduced the main features of the DOS and concluded that the phonon distribution is dominated by short-range interactions.

INFRARED ABSORPTION AND RAMAN SCATTERING

In amorphous solids the lack of translational symmetry and the absence of the momentum conservation rule in photon absorption and scattering has the consequence that

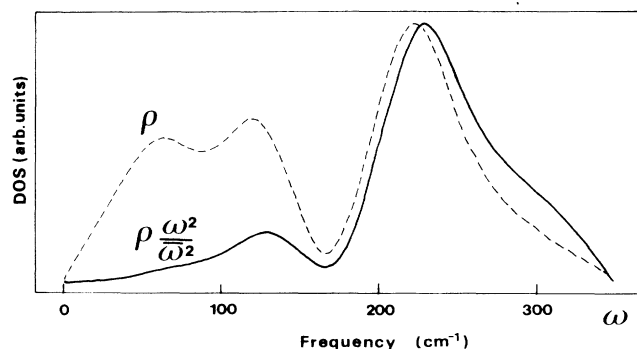


FIG. 1. Dashed line: Density of vibrational states (DOS) in amorphous arsenic as determined by Leadbetter *et al.* (Ref. 12). Continuous line: RDOS as given by the NN-CF model. $\bar{\omega}^2$ is the second moment of the DOS.

the phonon transitions explore the whole range of available states. The infrared and Raman spectra yield density of states profiles which are distorted by the frequency dependence of the matrix elements. The two principal bands observed in IR absorption in bulk amorphous arsenic¹³ are centered at 130 and 230 cm^{-1} and can be associated with the bending and stretching bands in the vibrational DOS. The Raman scattering in amorphous As has been measured by Lannin¹⁵ and his results are reported in Fig. 2. HH and HV refer to the polarizations of the incident and scattered light relative to the scattering plane. The Raman spectra separate into two main features: a strong peak centered at about 220 cm^{-1} and a weaker broader peak ranging from 60 to 150 cm^{-1} .

An interesting feature of Raman scattering in amorphous arsenic is the shift in the optical mode peak for different polarizations, an effect which usually is ascribed to some molecularlike character of the system. I_{HV} peaks near 230 cm^{-1} , corresponding to the maxima of the infrared absorption and of the neutron density of states, whereas I_{HH} has its maximum at about 200 cm^{-1} . This behavior has been studied in detail in Ref. 16 and the peak at 200 cm^{-1} has been attributed to the SS (symmetric stretching) vibrations which induce a strong polarized Raman activity.

As a result, the vibrational density of states of amorphous arsenic is better reproduced by I_{HV} than by I_{HH} , where matrix element effects mask the true DOS. The Raman intensity in amorphous systems is usually expressed in a form reduced by population factors for a better comparison with the phonon density of states:

$$I_R(\omega) = \frac{\omega}{n(\omega) + 1} I(\omega), \quad (14)$$

where $n(\omega)$ is the Bose-Einstein distribution function and $I(\omega)$ is the experimental intensity.

The reduced Raman intensity $I_R(\omega)$ can be written approximately as the product of the density of vibrational states $\rho(\omega)$ and a matrix element term

$$I_R(\omega) = R(\omega)\rho(\omega). \quad (15)$$

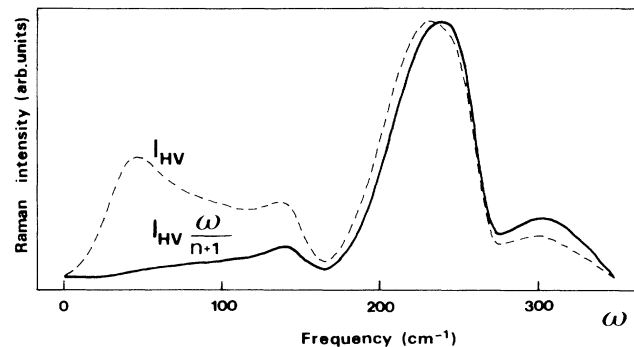


FIG. 2. Dashed line: Depolarized HV Raman intensity in amorphous arsenic as measured by Lannin (Ref. 15). Continuous line: Reduced Raman intensity [Eq. (13)] calculated at $T=300\text{ K}$ from Lannin's data. n is the Bose-Einstein population factor.

A best fit for the phonon density of states is usually looked for with $R(\omega) = \omega^n$ ($n = 1, 2, \dots$).¹⁵

RAMAN SCATTERING MECHANISMS

We will adopt the localized point of view of Alben *et al.*¹⁷ to express the Raman intensity in an amorphous system as a sum of local contributions from the bonds between the atoms in the random network. The Raman activity of a mode of frequency ω is given by the polarizability induced by the mode. Following Refs. 5, 14, and 16 we assume that the reduced Raman intensity at frequency ω is given by

$$I_R(\omega) = |\hat{\epsilon}_i \cdot \vec{D} \cdot \hat{\epsilon}_s|_{\omega}^2, \quad (16)$$

where \vec{D} is the vibrational polarizability tensor and $\hat{\epsilon}_i$ and $\hat{\epsilon}_s$ are the incident and scattered light polarization vectors, respectively. As in Refs. 14 and 17 we assume for \vec{D} the three independent local mechanisms corresponding to symmetry allowed contributions of pairs of identical atoms

$${}_1\vec{D} = \sum_{ll'} \{ \hat{\mathbf{R}}_{ll'} \hat{\mathbf{R}}_{ll'} - \frac{1}{3} \vec{I} \} \mathbf{u}_l \cdot \hat{\mathbf{R}}_{ll'}, \quad (17a)$$

$${}_2\vec{D} = \sum_{ll'} \{ \frac{1}{2} [\hat{\mathbf{R}}_{ll'} \mathbf{u}_l + \mathbf{u}_l \hat{\mathbf{R}}_{ll'}] - \frac{1}{3} \vec{I} \mathbf{u}_l \} \cdot \hat{\mathbf{R}}_{ll'}, \quad (17b)$$

$${}_3\vec{D} = \sum_{ll'} \vec{I} \mathbf{u}_l \cdot \hat{\mathbf{R}}_{ll'}. \quad (17c)$$

The sums in Eqs. (17) extend over all atoms l and their nearest neighbors l' ; $\hat{\mathbf{R}}_{ll'}$ is the unit vector from the equilibrium position of atom l to that of its neighbor l' . ${}_1\vec{D}$ and ${}_3\vec{D}$ have contributions only from bond-compression motions, while ${}_2\vec{D}$ contains contributions from bond bending and is usually small.^{5,17} ${}_3\vec{D}$ represents a change in the bond polarizability tensor proportional to the unit tensor and therefore it contributes only to the polarized spectrum. ${}_1\vec{D}$ is a traceless contribution which is diagonal if the z axis is the bond direction. For mechanisms ${}_1\vec{D}$ and ${}_2\vec{D}$ the depolarized scattering I_{HV} is $\frac{3}{4}$ of I_{HH} , while for ${}_3\vec{D}$ I_{HV} is zero.¹⁷ The scattering $I_{HH} - \frac{4}{3} I_{HV}$ (called pure polarized scattering) contains contributions only from mechanism ${}_3\vec{D}$.

In amorphous arsenic the ${}_3\vec{D}$ mechanism is particularly interesting as it is mainly due to symmetric stretching motions which give rise to anomalous molecular like peaks in the Raman polarized scattering.^{5,18} This mechanism has been shown to be responsible for the lower frequency peak in I_{HH} Raman scattering.¹⁶ The symmetric stretching motion corresponds, in a molecular picture, to the motion of As atoms along the perpendicular to the plane of the other three atoms coordinated to it. This SS motion has analogues in different random networks¹⁸ and it has been considered as responsible for strong and polarized Raman activity.

On the other hand, the Raman intensity for HV scattering, reduced by T dependent factors by Eq. (14), is directly connected to the density of vibrational states.^{5,14,16} We

then assume that ${}_3\vec{D}$ is responsible for I_{HH} whereas ${}_1\vec{D}$ is responsible for I_{HV} and approaches the density of states as given by a NN-CF model.

Therefore, to the extent that all bonds are similar and in the hypothesis of an incoherent superposition of the bond activities, on the basis of Eqs. (16) and (17a) we find that the (reduced) Raman intensity I_{HV} , due to mechanism ${}_1\vec{D}$, is proportional to the (average) square compression of the bonds. The main result is then that, being the relative local density of states contributing to EXAFS also given by the square compression of the bonds, we may write the following relation:

$$I_R(\omega) = A \rho_R(\omega), \quad (18)$$

where A is a normalization constant. This establishes the connection between reduced Raman intensities and EXAFS determined density of states.

In $a-Ge$ this relation has been verified by equation-of-motion calculations of both quantities in a CRN model.⁵ The results for the mechanism ${}_1\vec{D}$ are close to the RDOS, the low-frequency acoustic modes, which contribute very little to the bond compression, being effectively suppressed. We have tested these ideas in amorphous arsenic by reduction of Lannin's¹⁵ Raman data (see Fig. 2) obtaining a Raman deduced RDOS $\rho_R^R(\omega)$ and through Eq. (9) we have calculated the temperature dependence of σ_R^2 .

Moreover, we have tested the hypothesis that the NN-CF is a good approximation for arsenic, and then we have defined [see Eq. (10)] a neutron deduced RDOS $\rho_R^N(\omega)$

$$\rho_R^N(\omega) = \frac{\omega^2}{\bar{\omega}^2} \rho(\omega), \quad (19)$$

where $\rho(\omega)$ is the density of states determined by inelastic neutron scattering¹² and $\bar{\omega}^2$ is the second moment. Figure 1 shows both the experimental density of states and the calculated neutron RDOS.

We then have, at least in principle, two ways of obtaining relative density of states: from depolarized Raman data and from the neutron scattering spectrum. From Figs. 1 and 2 the close similarity between ρ_R^R and ρ_R^N is apparent. This is reflected in the first moments of the two RDOS (see Table I) and, due to the fact that the tempera-

TABLE I. First positive and negative moments (in cm^{-1}) of three relative vibrational densities of states (RDOS): ρ_R^R , deduced from nondiagonal Raman intensity I_{HV} [Eq. (14)]; ρ_R^N , obtained by Eq. (19) from inelastic scattering density of states; and ρ_R^D as given by a correlated Debye model (Eq. 12) with $\Theta_D = 283$ K. The Einstein frequency in the last row is the average between $(\bar{\omega}^{-1})_R^{-1}$ and $(\bar{\omega}^{-2})_R^{-1/2}$ [see Eq. (11)].

	ρ_R^R	ρ_R^N	ρ_R^D
$\bar{\omega}$	230.4	230.6	112.4
$(\bar{\omega}^2)^{1/2}$	236.6	237.5	137.3
$(\bar{\omega}^{-1})^{-1}$	207.8	207.8	219.1
$(\bar{\omega}^{-2})^{-1/2}$	183.8	186.6	176.4
ω_E	195.8	197.2	197.8

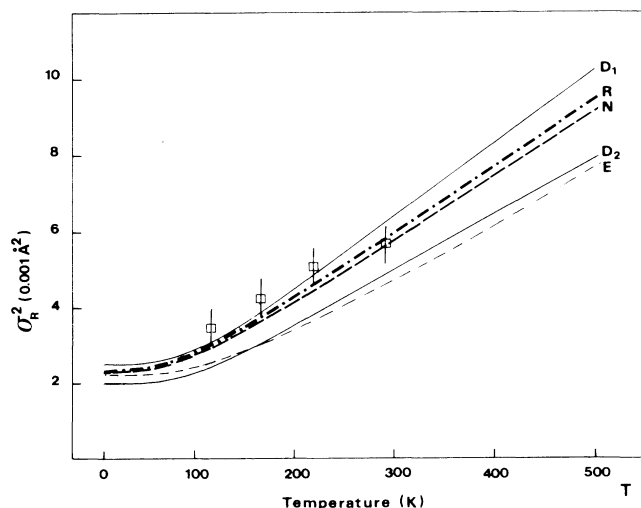


FIG. 3. Nearest-neighbor mean-square relative displacement σ_R^2 in amorphous arsenic as a function of the temperature. The squares are the experimental data obtained by Fontana *et al.* (Ref. 7) reported with the corresponding error bars. D_1 and D_2 refer to the correlated Debye model for $\Theta_D = 250$ and 320 K, respectively. The curve E is calculated from the Einstein model with an Einstein temperature $\Theta_E = \hbar\omega_E/k_B T = 300$ K. The dot-dashed and the dashed thick curves labeled R and N are the results of the calculation through Eq. (9) with Raman (ρ_R^R) and neutron (ρ_R^N) relative density of states, respectively.

ture dependence of the EXAFS Debye-Waller factor is mainly determined by the negative moments [Eq. (11)], we expect that these two density of states will give similar results.

DEBYE-WALLER FACTOR RESULTS

EXAFS measurements on the As K edge have been reported previously.⁷ The EXAFS data were taken at the PULS facility (INFN Laboratories, Frascati, Italy) using the synchrotron radiation from the ADONE storage ring. The temperature dependence of σ_R^2 was obtained by means of a fitting procedure in k space or by the ratio method² with respect to the low-temperature reference. The results are reported in Fig. 3. A least-squares fitting to the data with Eq. (4) (Einstein model) gives $\omega_E = 176$ cm^{-1} . A reasonable fit to the experimental data over a large temperature interval should be given by an Einstein model with the parameter ω_E taken as an average between $(\omega^{-1})_R^{-1}$ and $(\omega^{-2})_R^{-1/2}$. This prescription, using negative moments calculated from neutron and Raman reduced densities of states, gives the values reported in Table I. A correlated Debye model [Eq. (12)] gives a best fit to the

experimental data with a Debye temperature parameter $\Theta_D = \hbar\omega_D/k_B = 283$ K, which is in close agreement with the literature values.¹²

The temperature dependence of the EXAFS MSDR by using the Raman ρ_R^R and neutron ρ_R^N RDOS has been determined performing the integration in Eq. (9) from $\omega = 0$ to a cutoff frequency at 350 cm^{-1} , where the densities of states have been assumed equal to zero. The results of these calculations are shown in Fig. 3. We see that the temperature behavior of σ_R^2 obtained with these parameter-free relative densities of states is in good agreement with the experimental results.

CONCLUSIONS

In this work we have extended to amorphous arsenic the connection between the Raman-determined vibrational density of states and the EXAFS Debye-Waller disorder parameter σ_R^2 . In addition we have found that the temperature dependence of σ_R^2 is well reproduced, without fitting parameters, both by the relative density of states obtained from a Raman reduced VH intensity and by a neutron determined density of local states as given by a NN-CF model. These results stress the importance of the central bond-stretching forces in the vibrational dynamics of amorphous arsenic and show the possibility to check force constant models, to study average lattice dynamical properties on the basis of EXAFS results or to obtain information on the thermal disorder parameter from Raman spectra. The second moment of the phonon DOS may, for example, be measured in amorphous solids from the Raman spectra and compared with the results obtained in EXAFS σ_R^2 temperature dependence or by heat capacity data.⁶ For amorphous arsenic the simple dynamical model based on the bond-stretching mechanism gives a good estimate of the EXAFS MSDR. The disorder seems, therefore, essentially dynamic in character and the small difference with the experimental results could represent a contribution from static disorder which seems to decrease at higher temperatures where the molecular As_4 units could be more decoupled. However, to confirm this last hypothesis, further high-temperature measurements are needed.

ACKNOWLEDGMENTS

The author is indebted to Professor J. J. Rehr for his unpublished results, to Professor M. P. Fontana for stimulating discussions and to Dr. L. Oddi for useful suggestions. This work was supported by Gruppo Nazionale di Struttura della Materia, CNR, Italy and Unità di Firenze, Centro Interuniversitario di Struttura della Materia, Ministero della Pubblica Istruzione (Firenze, Italy).

¹G. Beni and P. M. Platzman, Phys. Rev. B **14**, 1514 (1976).

²W. Bohmer and P. Rabe, J. Phys. C **12**, 2465 (1979).

³E. Sevillano, H. Meuth, and J. J. Rehr, Phys. Rev. B **20**, 4908 (1979).

⁴R. B. Greggor and G. W. Lytle, Phys. Rev. B **20**, 4902 (1979).

⁵P. P. Lottici and J. J. Rehr, Solid State Commun. **35**, 565

(1980).

⁶G. S. Knapp, H. K. Pan, and J. M. Tranquada, Phys. Rev. B **32**, 2006 (1985).

⁷M. P. Fontana, P. P. Lottici, C. Razzetti, D. Bianchi, G. Antonioli, and U. Emiliani, Solid State Commun. **43**, 561 (1982).

⁸EXAFS Spectroscopy: Techniques and Applications, edited by

- B. K. Teo and D. C. Joy (Plenum, New York, 1981).
- ⁹G. Bunker, Nucl. Instrum. Methods **207**, 437 (1983).
- ¹⁰J. J. Rehr (unpublished).
- ¹¹G. N. Greaves, S. R. Elliott, and E. A. Davis, Adv. Phys. **28**, 49 (1979).
- ¹²A. J. Leadbetter, P. M. Smith, and P. Seyfert, Philos. Mag. **33**, 441 (1976).
- ¹³G. Lucowsky and J. C. Knights, Phys. Rev. B **10**, 4324 (1974).
- ¹⁴D. Beeman and R. Alben, Adv. Phys. **26**, 339 (1977).
- ¹⁵J. S. Lannin, Phys. Rev. B **15**, 3863 (1977).
- ¹⁶P. P. Lottici, Phys. Status Solidi B **122**, 431 (1984).
- ¹⁷R. Alben, D. Weaire, J. E. Smith, Jr., and M. H. Brodsky, Phys. Rev. B **11**, 2271 (1975).
- ¹⁸P. N. Sen and M. F. Thorpe, Phys. Rev. B **15**, 4030 (1977).